Desalination and Water Treatment
www.deswater.com

doi: 10.5004/dwt.2018.22665

118 (2018) 294–303
June

Modeling the calcium and magnesium removal from seawater by immobilized biomass of ureolytic bacteria *Bacillus subtilis* through response surface methodology and artificial neural networks

Dayana Arias[a,b], Mariella Rivas[a,c], Ricardo Guiñez[d], Luis A. Cisternas[b,c,*]

[a]*Laboratorio de Biotecnología Algal y Sustentabilidad (BIOAL), Facultad de Ciencias del Mar y Recursos Biológicos, Universidad de Antofagasta, Av. Angamos 601, Antofagasta, Chile, Tel. +56 55 3211522; email: dayana.arias@uantof.cl (D. Arias)*
[b]*Departamento de Ingeniería Química y Procesos de Minerales, Universidad de Antofagasta, Av. Angamos 601, Antofagasta, Chile, Tel. +56 55 2 637 323; email: luis.cisternas@uantof.cl (L.A. Cisternas)*
[c]*Centro de Investigación Científico Tecnológico para la Minería (CICITEM), Av. José Miguel Carrera 1701, Antofagasta, Chile, Tel. +56 55 2 220 647; email: mariella.rivas@cicitem.cl (M. Rivas)*
[d]*Instituto de Ciencias Naturales Alexander Von Humboldt, Facultad de Ciencias del Mar y Recursos Biológicos, Universidad de Antofagasta, Av. Angamos 601, Antofagasta, Chile, Tel. +56 55 2 637 401; email: ricardo.guinez@uantof.cl (R. Guiñez)*

Received 5 March 2018; Accepted 25 June 2018

ABSTRACT

In this work, response surface methodology (RSM) and artificial neural networks were applied for modeling the removal of Ca^{2+} and Mg^{2+} from seawater by immobilized biomass in polyvinyl alcohol-alginate spheres of the ureolytic bacterium *Bacillus subtilis* strain LN8B. RSM was developed by considering a three-level factorial design with three input variables, that is, concentration of urea, number of cells in the immobilization matrix, and seawater to spheres ratio (SW:S). At the same time, a radial basis function networks (RBFNs) were used for a better representation of the removal of Ca^{2+} and Mg^{2+} and compared with RSM. It was found that all variables considered have important effects on both of Ca^{2+} and Mg^{2+} removal from seawater. Based on an analysis of variance of a three-level factorial design it was determined that urea concentration, number of cells, and SW:S were highly significant in the removal of calcium. In addition, the quadratic term of urea concentration, interaction urea concentration with number of cells, and interaction number of cells with SW:S ratio were significant in calcium removal. For magnesium removal, the number of cells was the only highly significant variable, whereas the urea concentration, SW:S, and quadratic term of number of cells were significant. The results demonstrated that RBFNs gave better modeling capability than RSM.

Keywords: Seawater; Response surface methodology; Radial basis function networks; Ureolytic bacteria; Biomineralization

1. Introduction

The scarcity of water resources in arid, semi-arid, and hyper-arid zones has generated the need to seek other nontraditional sources of water resources. Desalination of seawater (SW) has emerged as a feasible solution. According to International Desalination Association by June 30, 2015 there are 18,426 desalination plants in 159 countries, the global capacity of commissioned desalination plants is more than 86.8 million m^3 d^{-1}, and more than 300 million people rely on desalinated water for some or all their daily needs [1]. Desalinated SW is used for human consumption and industrial uses. However, the water quality required for different applications is not the same. For example, boron in Mediterranean SW after reverse osmosis (RO) reaches 2 mg L^{-1}, which does not constitute a threat to human health but is toxic for all but the most tolerant crops [2]. On the other hand, desalination removes ions that are essential to plant growth.

* Corresponding author.

Ca^{2+} and Mg^{2+} in SW cause problems in various industrial operations. These ions are the major components of scaling in operations such as RO unit [3–5], heating unit of multistage flash distillation [6], membrane distillation for desalination applications [7], cooling water systems of power generation [8], and water injection operation of oil and gas production [9]. The application of SW in the flotation of copper and molybdenum minerals has been carried out using RO desalted water and using raw SW [10]. Desalination produces water without ions that do not generate major changes in traditional flotation processes. However, the cost and eventual generation of greenhouse gases from energy generation for RO desalination is a problem. The presence of ions in SW facilitates flotation because the enhancement of the floatability for surfaces that are already hydrophobic, reduction of the bubbles size, improve froths stability, among other reasons [11]. However, the presence of Ca^{2+} and Mg^{2+} ions reduces the recovery of minerals such as chalcopyrite (copper) and molybdenite (molybdenum) by the precipitation of colloid of Mg and Ca [12,13]. For this reason, several studies have analyzed the flotation with pretreated SW to remove Mg and Ca [14]. Studies have shown that the behavior of treated SW flotation processes is more efficient, the pretreatment costs are much lower than the RO desalination, and the environmental impact is lower than the RO desalination. There are no mining companies that perform a partial distillation of the SW to leave those elements harmless to the processes eliminating those harmful. In summary, the removal of magnesium and calcium from SW can be an important alternative to the use of SW in several industries.

An alternative for removal of Ca^{2+} and Mg^{2+} ions is the application of biological precipitation processes or biomineralization based on the hydrolysis of urea. Biomineralization has been extensively described in the application of soil biocementation [15–17], restoration of monuments and limestone statues, production of biocement, removal of soluble contaminants such as heavy metals and radioactive elements [18,19], and removal of calcium from industrial wastewater [20]. These processes represent an interesting alternative for pretreatment of SW, industrial wastewaters, hard water, and groundwater with excessive levels of contaminants such as heavy metals, radionuclides, phosphates, and salts [21–24]. One of the earliest studies described by Hammes et al. [20] determined the removal of calcium by biomineralization from industrial wastewater (Ca^{2+} 500–1,500 mg L^{-1}) through the use of a semicontinuous reactor removing about 90% of calcium from a paper recycling facility. A recent study [25] has analyzed biomineralization as potential pretreatment technology to SW due to the ability of ureolytic strains to precipitate ions from SW. In this publication, the bacterium *Rhodococcus erythropolis* was able to precipitate a ~95% soluble calcium and 8% magnesium by enzymatic hydrolysis of urea. The analysis of crystals showed that correspond to ~12.69% monohydrocalcite, ~30.72% struvite, and ~56.59% halite. The microbial urease enzyme hydrolyzes urea to produce dissolved ammonium, dissolved inorganic carbon and CO_2, and the ammonia released in the surroundings subsequently increases pH, leading to accumulation of insoluble biominerals according to the ions present in the medium [18].

The precipitation of ions from SW by ureolytic bacteria depends on various factors such as initial urea concentration, reaction temperature, the initial ion concentration, ionic strength, the pH, the type and bacterial cell concentration as well as its free or immobilized state [26,27]. Response surface methodology (RSM) is a collection of mathematical and statistical techniques for modeling and optimization of processes, products, and experiment results [28]. This includes several separation processes [29,30]. In RSM an experimental design is used to determine the significant factors that affect an experiment. The data obtained in these experiments can be used to develop empirical models, which can be used to search better experiment results. In RSM linear or square polynomial functions are used as mathematical models. However, many times the experimental data do not adequately fit those polymorphic functions, in which case artificial neural networks (ANNs) may be a better option [31,32]. The ANN, which is based on the human brain, establishes a complex nonlinear relationship between dependent and independent factors without knowledge on the relationship of variables [33]. There are several types of ANNs including radial basis function networks (RBFNs) and multilayer perceptrons. In work developed by Charte et al. [31], a comparative study was made including RBFN, multilayer perceptrons, a support vector machine, and a fuzzy system together with the RSM approach. They concluded that RBFN performs better, with statistically significant differences, and RSM was the second-best method. An RBFN consists of an input layer, hidden layer, and output layer with the activation function of the hidden units being radial basis functions [34]. To model and optimize effective ion removal parameters with a reasonable number of experiments, the application of experimental design methodologies together with ANNs may be useful.

The objective of this work is to study the effect of urea concentration, number of cells in the immobilization matrix, and ratio of SW to spheres (SW:S) on the removal of Ca^{2+} and Mg^{2+} from SW by immobilized biomass in polyvinyl alcohol-alginate (PVA-Al) spheres of the ureolytic bacterium *Bacillus subtilis*. RSM and RBFN are used for modeling the removal of Ca^{2+} and Mg^{2+}.

2. Experimental and modeling

2.1. Microorganism, growing conditions, and obtaining of biomass

B. subtilis strain LN8B (KX018264.1) was used, which was isolated from Laguna Salada (San Pedro de Atacama, Chile). To obtain biomass, the cells were cultured in LM medium consisting of Luria broth (MoBio Lab., Inc., USA) dissolved in SW, incubated at 30°C at 120 rpm agitation and then harvested by centrifugation at 4,000 rpm for 20 min.

2.2. Biomass immobilization in PVA-Al beads

Concentrated *B. subtilis* strain LN8B cells were mixed with a polyvinyl alcohol solution (Sigma-Aldrich, Mw 89,000–98,000, 99+% hydrolyzed) at 12% and an alginic acid solution (Sigma-Aldrich, USA) at 2%, to a final concentration of 1×10^9, 1×10^{10}, and 1×10^{11} cells mL^{-1}. The mixture was dripped via a peristaltic pump into a sterile solution of 4% calcium chloride (Merck, Germany) and 4% boric acid (Merck) for 2 h to form immobilized cell spheres of 0.4 cm diameter.

After 2 h, the spheres were washed three times with sterile distilled water and stored at 4°C until use. Spheres without bacteria and spheres with bacteria and without urea were used as control.

2.3. Batch removal experiments

The Ca^{2+} and Mg^{2+} removal studies were performed in 250 mL Erlenmeyer flasks at an incubation temperature of 30°C and a constant shaking of 120 rpm for 2 weeks. The analyzed input factors correspond to the concentration of urea (between 20 and 40 g L^{-1}), cellular concentration (the concentrations are expressed in logarithmic scale, pC = Log (cells mL^{-1}), between 9 and 11), and SW:S (between 1 and 3). The total volume, SW plus spheres, was 100 mL.

2.4. Analysis method and X-ray diffraction analysis

The quantification of Ca^{2+} and Mg^{2+} was determined by atomic absorption and corroborated by the Merck kits 1.14815.0001 and 1.00815.0001, respectively. NaCl concentration was measured by a digital refractometer. The quantification of ammonia was performed according to what was described by Arias et al. [25], and the pH was determined with the pH meter HA 1230B (Hanna Instruments, Italy).

X-ray diffraction (XRD) analyses were obtained using a diffractometer (Siemens D5000) with a secondary graphite monochromator and CuKα radiation. The data were collected during an integration time of 1.0 s in steps of 0.02° 2θ to 40 kV and 30 mA and scanning from 3° to 70° 2°. The simple components were identified by comparing them with the standards established by the International Diffraction Data Center.

2.5. Design of experiment

In this study, the three-level full factorial design (3^3 design) was selected for the modeling of removal of Mg^{2+} and Ca^{2+} from SW. Usually, it is considered that three-level full factorial design is prohibitive in terms of number of runs, and thus regarding cost and effort. However, for three input factors, only 27 runs are needed, and the design provides more data for modeling possible curvature in the behavior of the output variables. This method, as well as other more efficient experimental design methods such as central composite design, is suitable for fitting a quadratic surface as well as to analyze the interaction between parameters. However, 3^3 design can be more appropriate when ANNs are used because the sample size can affect the fitting results [35].

A quadratic model corresponding to the following second-order equation, but in terms of the significant input factors, was built to describe the Mg^{2+} and Ca^{2+} removal:

$$Y = b_0 + b_1X_1 + b_2X_2 + b_3X_3 + b_{11}X_1^2 + b_{22}X_2^2 + b_{33}X_3^2 + b_{12}X_1X_2 + b_{13}X_1X_3 + b_{23}X_2X_3 \quad (1)$$

where Y is the Mg^{2+} or Ca^{2+} removal, and X_i are the input factors. b_0 is the constant coefficient, b_i with i = 1,2,3 are linear coefficients, b_{ii} with i = 1,2,3 are the quadratic coefficients, and b_{ij} with i and j = 1,2,3; $i \neq j$ are the interaction coefficients.

The statistical significance of the models was justified through analysis of variance (ANOVA) for a polynomial model with 95% confidence level. The quality of the fit polynomial model was expressed by the coefficient of determination R^2, but the root mean square (RMS), mean absolute error (MAE), and mean relative error (MRE) were also determined using the following equations:

$$\mathrm{RMS} = \sqrt{\frac{\sum_i \left(Y_i^{\mathrm{Exp}} - Y_i^{\mathrm{Cal}}\right)^2}{n}} \quad (2)$$

$$\mathrm{MAE} = \frac{\sum_i \left|Y_i^{\mathrm{Exp}} - Y_i^{\mathrm{Cal}}\right|}{n} \quad (3)$$

$$\mathrm{MRE} = \frac{\sum_i \left|Y_i^{\mathrm{Exp}} - Y_i^{\mathrm{Cal}}\right| / Y_i^{\mathrm{Exp}}}{100n} \quad (4)$$

The levels of the factors were selected according to the literature and our preliminary experience. The experimental factors and their levels are given in Table 1. The levels of input factors were defined based on previous results.

2.6. Radial basis function networks

Fig. 1 shows an RBFN, this considers a simple three layers network: input layer, hidden layer, and output layer. The first layers receive and transmit signs to neurons at hidden layer. In the hidden layer, the neurons calculate its output using radial basis functions. Finally, the output layer supplies the response of the neural network from the pondered linear combination of the activation of the hidden neurons; this combination has the next form [36]:

$$F(x) = \sum_{j=1}^{M} W_j \phi_j(x) \quad (5)$$

where M is the hidden neurons number, $x \in \mathbb{R}^p$ is the input, W_j are the weights, and $\varphi_j(x)$ is the Gaussian radial function, that is, it's a function whose values depend only on the distance of vector x respect of some vector $c_j \in \mathbb{R}^p$ fix,

$$\phi_j(x) = e^{\left(\frac{\|x - c_j\|^2}{\sigma_j^2}\right)} \quad (6)$$

where c_j and σ_j are the centers and width, respectively, of the jth hidden neural, and $\|.\|$ denotes the Euclidean distance.

The RBFN should be trained to obtain a specific goal. The learning procedure of an RBFN mainly includes two parts:

Table 1
Input factors and their levels

Factors	Symbol	Levels		
		Low	Intermediate	High
Urea concentration (g L^{-1})	X_1	20	30	40
pC = Log (cells mL^{-1})	X_2	9	10	11
SW:S	X_3	1	2	3

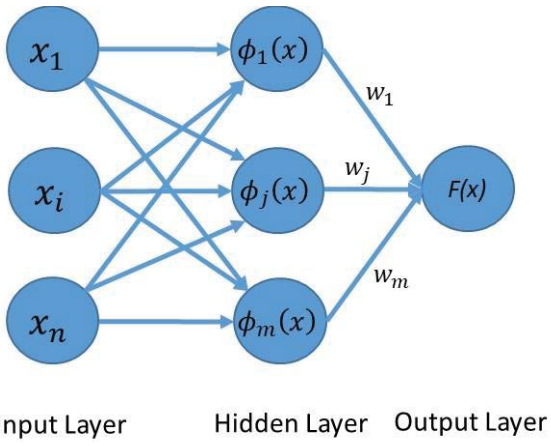

Fig. 1. Radial basis function networks.

one is the adjustment of the connection weight, and the other is the modification of center and width of hidden neurons. This training was performed using MathLab. If the MAE of prediction was higher than desired error, then the network topology was modified, center and width of the radial functions, and again were adjusted the connection weights. This procedure was repeated until to obtain a mean absolute desired error.

3. Results and discussion

3.1. Design of experiment

The results of calcium removal were analyzed on the 8th day, while those of magnesium on day 16. Sampling days were defined based on previous results that show that the process of calcium removal is faster than the removal of magnesium. Previous analyses by XRD indicated that calcium is precipitated mainly as monohydrate calcite ($CaCO_3 \cdot H_2O$) and magnesium as struvite ($NH_4MgPO_4 \cdot 6H_2O$). No precipitate formations were observed in controls (data not shown). Table 2 shows the results of calcium removal at day 8 including the experimental values of the pH and ammonium concentration. According to the ureolytic metabolism, this process is explained because *B. subtilis* strain LN8B hydrolyzes urea to produce dissolved ammonium, dissolved inorganic carbon and CO_2, and the ammonia released in the surroundings subsequently increases pH, leading to accumulation of insoluble $CaCO_3$ either hydrated or anhydrous in a calcium-rich environment like SW [26]. Therefore, ammonium concentrations were measured because it indicates

Table 2
Results on calcium removal at day 8

Exp	Urea (g L^{-1})	pC	SW:S	Calcium (mg L^{-1})	pH	Ammonium (mg L^{-1})	Calcium removal (%)
1	20	9	1	392	5.9	271	0.7
2	20	9	2	392	6.44	272	0.7
3	20	9	3	327	6.49	157	17.2
4	20	10	1	392	6.18	338	0.7
5	20	10	2	360	6.59	299	9.0
6	20	10	3	233	7.11	403	41.0
7	20	11	1	392	7.91	426	0.7
8	20	11	2	280	8.91	770	29.1
9	20	11	3	106	9.03	1,033	73.1
10	30	9	1	392	6.39	234	0.7
11	30	9	2	392	6.31	245	0.7
12	30	9	3	371	6.54	224	6.0
13	30	10	1	357	6.39	332	9.7
14	30	10	2	324	7.13	275	17.9
15	30	10	3	280	7.85	522	29.1
16	30	11	1	307	8.68	1,024	22.4
17	30	11	2	133	9.06	1,583	66.4
18	30	11	3	88	9.14	1,357	77.6
19	40	9	1	392	6.39	179	0.7
20	40	9	2	392	6.38	276	0.7
21	40	9	3	245	6.65	257	38.1
22	40	10	1	215	6.45	418	45.5
23	40	10	2	183	7.57	507	53.7
24	40	10	3	103	8.28	371	73.9
25	40	11	1	80	8.83	1,461	79.9
26	40	11	2	6	9.02	2,039	98.6
27	40	11	3	0	9.16	1,439	100.0

the level of urea hydrolysis, and the pHs were determined because they indicate the ureolytic activity of bacteria. Fig. 2 shows the typical behavior of the pH variation during days 1–16. Exp 1 (see the first column in Table 2) corresponds a case with low removal of calcium (0.7%), Exp 6 represents a case with moderate removal of calcium (41%), and Exp 27 characterizes a case with high removal of calcium (100%). Similar pH profiles were observed in all experiments, but the removal of calcium also depends on other variables. In Fig. 3 the correlation between calcium removal and pH at day 8 is exposed. There is a good correlation, almost linear when the urea concentration is 40 g L^{-1} (correlation coefficient 0.9299), but that correlation decreases as the urea concentration decreases. Note that the pH does not exceed 9.3 due to the equilibrium of the ammonium buffer ($NH_4^+ \leftrightarrow NH_3 + H^+$).

In Fig. 4 the correlation between calcium removal and ammonium concentration at day 8 is presented. It is observed that the highest calcium removals occur when the ammonium concentration is high. The correlation is not linear, but rather logarithmic with the ammonium concentration (correlation coefficient 0.8820 at 40 g urea L^{-1}). These results suggest that the relationship between pH and calcium removal is rather of solid–liquid equilibrium with high kinetics. That is, the precipitation of calcium is due to the change in pH. In contrast, the relationship between the amount of calcium removal and the ammonium concentration may be more related to a kinetic phenomenon in the process of urea hydrolysis.

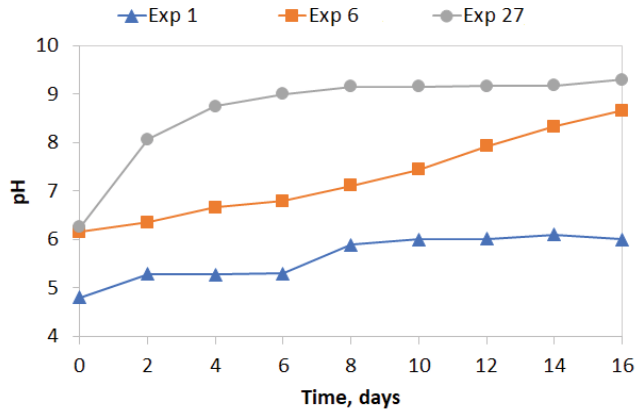

Fig. 2. Typical behavior of the pH variation during days 1–16.

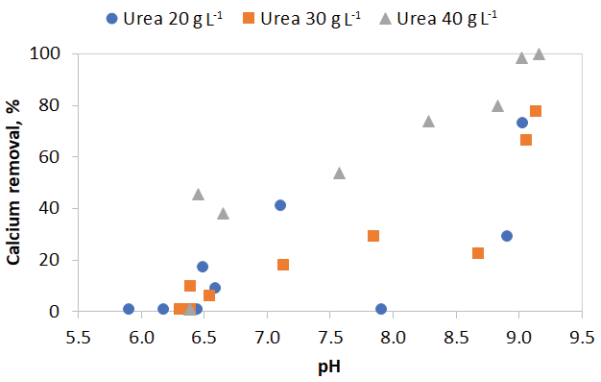

Fig. 3. Correlation between calcium removal and pH at day 8.

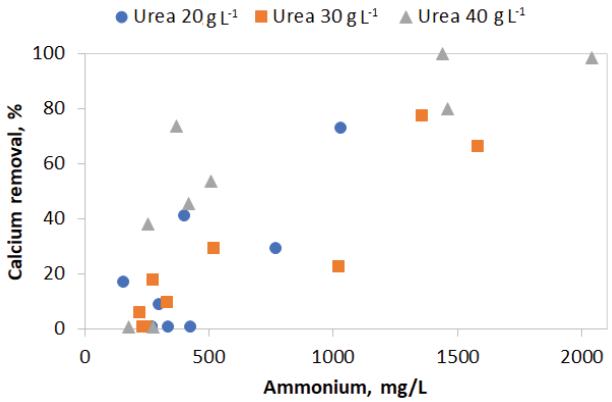

Fig. 4. Correlation between calcium removal and ammonium concentration at day 8.

Table 3 shows the results of magnesium removal at day 16 together with the values of pH, ammonium concentration, and chloride concentration. The removal of chloride, which precipitates as halite, is also included. The correlation with the pH and ammonium concentration is not clear, and therefore no conclusions can be obtained. However, it is observed that those experiments with less magnesium removal correspond to those with an SW:S ratio of 3 (Figs. 5 and 6). When urea concentration increases, the calcium and magnesium removal increases. However, an inverse relationship between the SW:S ratio in magnesium removal at day 16 and calcium removal at day 8 is observed (Fig. 7).

The elimination of magnesium by *B. subtilis* strain LN8B is due to the production of NH_4^+ product of urea hydrolysis, which produces in the presence of the dissolved magnesium ions in SW a magnesium precipitate as $NH_4MgPO_4{\cdot}6H_2O$ or struvite. When Mg^{2+} is abundant, struvite can be formed if the nitrogen and phosphorous concentrations are enough, and there is less calcium carbonate and/or magnesium [37].

The greatest removal was obtained in Exp 26 (87%), while the lowest was in Exp 3 (40.2%) in 16 d of testing. In spite of the good results, it is necessary to emphasize that the struvite precipitation depends on a minimum molar radius of 1:1:1 of Mg^{2+}:NH_4^+:PO_4^{3-} [38], therefore, the concentration of phosphate (PO_4^{3-}) influence the removal of magnesium.

3.2. Statistical analysis using ANOVA

The quadratic RSM adequacy and significance was checked using ANOVA. Table 4 shows the results of ANOVA analysis for the removal of calcium. Larger *F* values and smaller *P* values are an indication of the significance of the model. The model *P* value <0.0001 implied the high significance of the model, and *P* value <0.05 indicates that the term is significant. In this case, the input variable urea concentration, pC, and SW:S were highly significant. The quadratic term of urea concentration, interaction urea concentration with pC, and interaction pC with SW:S ratio were significant. The coefficient of determination (R^2) is defined as the ratio of the explained variable to the total variation and a measure of the degree of fit. It was found that the predicted values matched the experimental values well with $R^2 = 0.9385$. This implied that 93.85% of the variation for calcium removal

Table 3
Results on magnesium removal at day 16

Exp	Urea (g L^{-1})	pC	SW:S	Magnesium (mg L^{-1})	pH	Ammonium (mg L^{-1})	Chloride (mg L^{-1})	Magnesium removal	Chloride removal
1	20	9	1	807.5	5	56	20,800	44.3	9.6
2	20	9	2	830	5.21	59	19,000	42.8	17.4
3	20	9	3	867.5	6.26	37	20,600	40.2	10.4
4	20	10	1	550	6.39	209	20,400	62.1	11.3
5	20	10	2	507	7.48	341	20,500	65.0	10.9
6	20	10	3	837	8.67	538	23,000	42.3	0.0
7	20	11	1	405	8.91	1,273	19,700	72.1	14.3
8	20	11	2	442.5	9.15	1,255	19,800	69.5	13.9
9	20	11	3	612.5	9.19	1,117	18,600	57.8	19.1
10	30	9	1	710	6.45	148	23,000	51.0	0.0
11	30	9	2	782.5	6.45	64	23,000	46.0	0.0
12	30	9	3	800	6.92	130	23,000	44.8	0.0
13	30	10	1	240	6.99	424	18,000	83.4	21.7
14	30	10	2	530	6.31	163	16,900	63.4	26.5
15	30	10	3	400	9.11	858	14,600	72.4	36.5
16	30	11	1	337	9.01	1,500	15,000	76.8	34.8
17	30	11	2	400	9.18	1,789	13,000	72.4	43.5
18	30	11	3	647	9.2	1,637	22,400	55.4	2.6
19	40	9	1	702.5	6.54	95	18,100	51.6	21.3
20	40	9	2	715	6.91	180	14,700	50.7	36.1
21	40	9	3	825	7.58	299	16,800	43.1	27.0
22	40	10	1	365	7.77	701	19,000	74.8	17.4
23	40	10	2	400	8.95	835	21,200	72.4	7.8
24	40	10	3	430	9	1,152	21,300	70.3	7.4
25	40	11	1	292	9.17	1,575	21,300	79.9	7.4
26	40	11	2	188	9.23	2,027	20,800	87.0	9.6
27	40	11	3	384	9.3	1,765	17,800	73.5	22.6

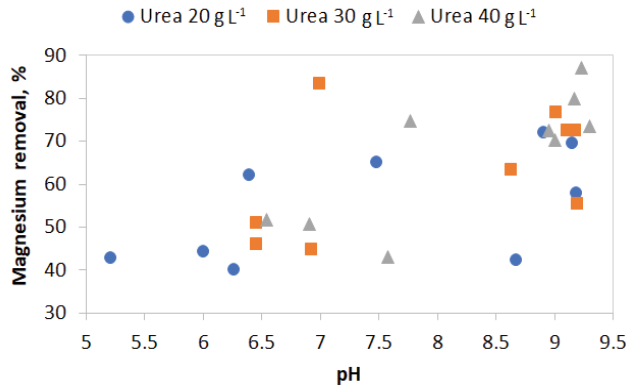

Fig. 5. Correlation between magnesium removal and pH at day 16.

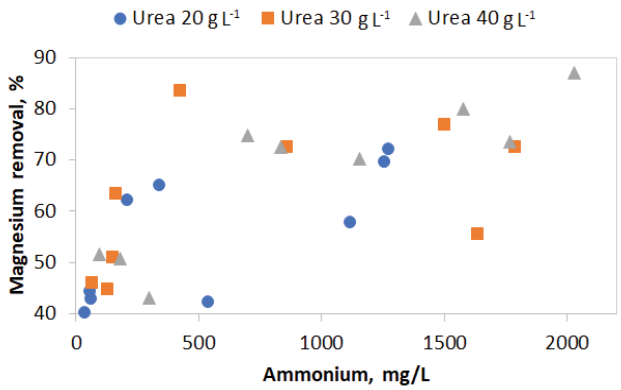

Fig. 6. Correlation between magnesium removal and ammonium concentration at day 16.

was explained by the independent variables and this also meant that the model did not explain 6.15% of the variation. The R^2 of 0.9385 was in reasonable agreement with adjusted for d.f. R^2 of 0.9059, also indicating reasonable predictability of the model.

Table 5 shows the results of ANOVA analysis for the removal of magnesium. In this case, the input variable pC was the only highly significant, whereas the input variables urea concentration and SW:S were significant. The quadratic term of pC was also significant. None of the interactions are

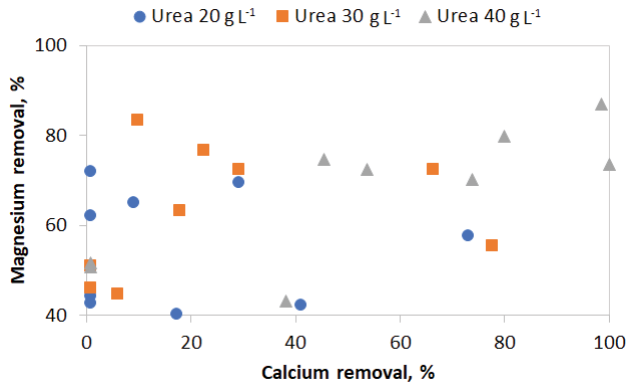

Fig. 7. Correlation between magnesium removal at day 16 and calcium removal at day 8.

significant. It was found that the predicted values matched the experimental values in a modest way with R^2 = 0.8763. Therefore, only 87.63% of the variation for magnesium removal was explained by the independent variables and the model did not explain 12.37% of the variation. The R^2 of 0.8762 and adjusted for d.f. R^2 of 0.8108 are in reasonable agreement.

3.3. Development of model regression equation

Based on the experimental design (Tables 2 and 3) and the ANOVA results (Tables 4 and 5), the quadratic RSM relating the calcium (Y(Ca)) and magnesium (Y(Mg)) removal with urea concentration (X_1), logarithm of cell concentration (X_2), and SW:S (X_3) was constructed to fit the experimental data. The models can be written as follows:

$$Y(\mathrm{Ca}) = b_0 + b_1X_1 + b_2X_2 + b_3X_3 + b_{11}X_1^2 + b_{12}X_1X_2 + b_{23}X_2X_3 \quad (7)$$

$$Y(\mathrm{Mg}) = b_0 + b_1X_1 + b_2X_2 + b_3X_3 + b_{22}X_2^2 \quad (8)$$

where b_0 = 635.1394403, b_1 = –98.72122053, b_2 = –14.27128156, b_3 = –68.21209661, b_{11} = 3.127796817, b_{12} = 1.58569795, and b_{23} = 7.579122003 for calcium removal. The following values for the accuracy metrics were obtained: RMS 10.11, MAE 8.72, and MRE 14.75. For magnesium removal the coefficient values are b_0 = –921.925288, b_1 = 0.596743297, b_2 = 183.6475097,

Table 4
Analysis of variance (ANOVA) for the response surface quadratic model of calcium removal

Source	Sum of squares	d.f.	Mean square	*F*-Ratio	*P*-Value	Significant
X_1 (urea)	5,688.89	1	5,688.89	54.59	0.0000	High
X_2 (pC)	12,853.4	1	12,853.4	123.35	0.0000	High
X_3 (SW:S)	4,769.39	1	4,769.39	45.77	0.0000	High
X_1X_1	770.667	1	770.667	7.40	0.0146	Yes
X_1X_2	2,002.08	1	2,002.08	19.21	0.0004	Yes
X_1X_3	154.083	1	154.083	1.48	0.2406	Not
X_2X_2	48.1667	1	48.1667	0.46	0.5057	Not
X_2X_3	675.0	1	675.0	6.48	0.0209	Yes
X_3X_3	73.5	1	73.5	0.71	0.4127	Not
Total error	1,771.5	17	104.206			
Total (corr.)	28,806.7	26				

Table 5
Analysis of variance (ANOVA) for the response surface quadratic model of magnesium removal

Source	Sum of squares	d.f.	Mean square	*F*-Ratio	*P*-Value	Significant
X_1 (urea)	660.056	1	660.056	17.02	0.0007	Yes
X_2 (pC)	2,913.39	1	2,913.39	75.12	0.0000	High
X_3 (SW:S)	522.722	1	522.722	13.48	0.0019	Yes
X_1X_1	15.5741	1	15.5741	0.40	0.5347	Not
X_1X_2	44.0833	1	44.0833	1.14	0.3013	Not
X_1X_3	27.0	1	27.0	0.70	0.4157	Not
X_2X_2	411.13	1	411.13	10.60	0.0047	Yes
X_2X_3	44.0833	1	44.0833	1.14	0.3013	Not
X_3X_3	31.1296	1	31.1296	0.80	0.3828	Not
Total error	659.352	17	38.7854			
Total (corr.)	5,328.52	26				

b_3 = –5.340996168, and b_{22} = –8.544061308. The values for the accuracy metrics are RMS 5.54, MAE 4.12, and MRE 7.12.

3.4. RBFN model

The structure and optimum values of RBFN parameters for both calcium and magnesium removal were determined using different number of hidden layer until to reach an RMS less than 1. In the RBFN used for the calcium removal, the architecture 3-21-1 (with 21 neurons in the hidden layer) of an RBFN an MSE of 0.3 was obtained. It was found that the predicted values matched the experimental values in very good with R^2 = 0.9999. Therefore, 99.99% of the variation for calcium removal was explained by the independent variables. The R^2 of 0.99799 and adjusted for d.f. R^2 of 0.9998 agree. The following values for the accuracy metrics were obtained: MAE 0.31, and MRE 0.27. These results are much better than those obtained with RSM. This is clearly shown in Fig. 8(a), which compares the experimental values versus the values predicted by RSM and RBFN.

In the RBFN used for the magnesium removal, the architecture 3-13-1 of an RBFN, an RMS of 4.82 was obtained. It was not possible to find a better ANN because at lower MSE values the response surface showed poor interpolation (oscillations). It was found that the predicted values matched the experimental values with R^2 = 0.9396 and in agreement with adjusted for d.f. R^2 of 0.9286, which is an improvement compared with RSM. The following values for the accuracy metrics were obtained: MAE 3.52 and MRE 0.06. These results are better than those obtained with RSM, which is clearly shown in Fig. 8(b).

Response surfaces were constructed using RBFN because RBFN gives better results and the form of response surfaces given by RBFN does not correspond to the typical quadratic model. Usually, the best results were obtained at high urea concentrations. However, these conditions mean higher costs because higher concentrations of urea mean higher consumption of this chemical reagent. Therefore, the response surfaces were constructed considering medium values of urea (30 g L^{-1}). High values of SW:S gives high removal of calcium but low removal of magnesium, and vice versa. Also, low ratios of SW:S means larger reactors. The response surfaces were constructed considering a value of 2 for SW:S.

High values of urea concentration mean better calcium removals as can be seen in Fig. 9. An economic evaluation between the cost of urea and the time to remove calcium is necessary to make an informed decision. High values of pC can help obtain good results for calcium (Fig. 9) and magnesium (Fig. 10). High values of SW:S favor the removal of calcium and low values favor the removal of magnesium

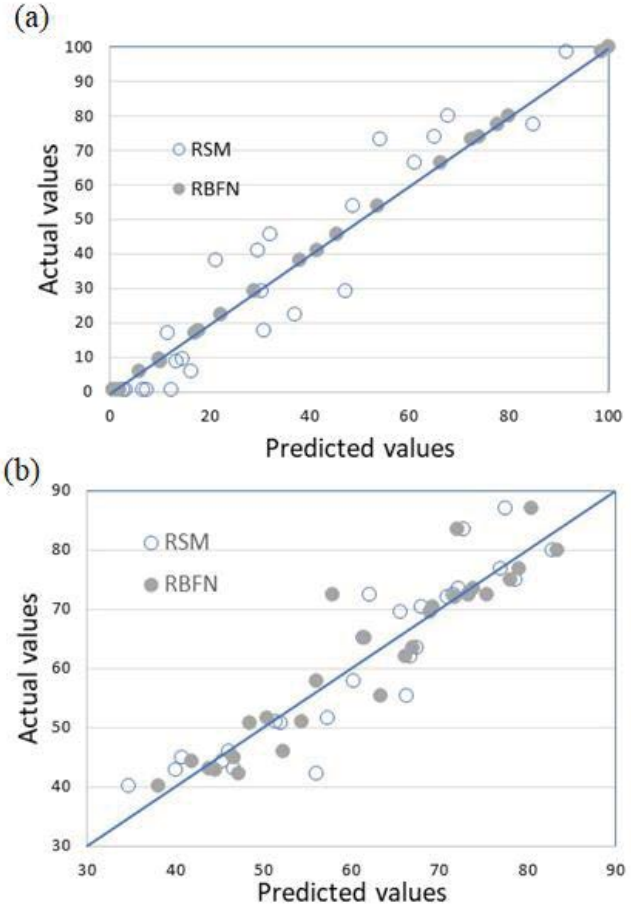

Fig. 8. Experimental data versus predicted data given by RSM and RBFN for calcium and magnesium removal. Calcium removal (a) and magnesium removal (b).

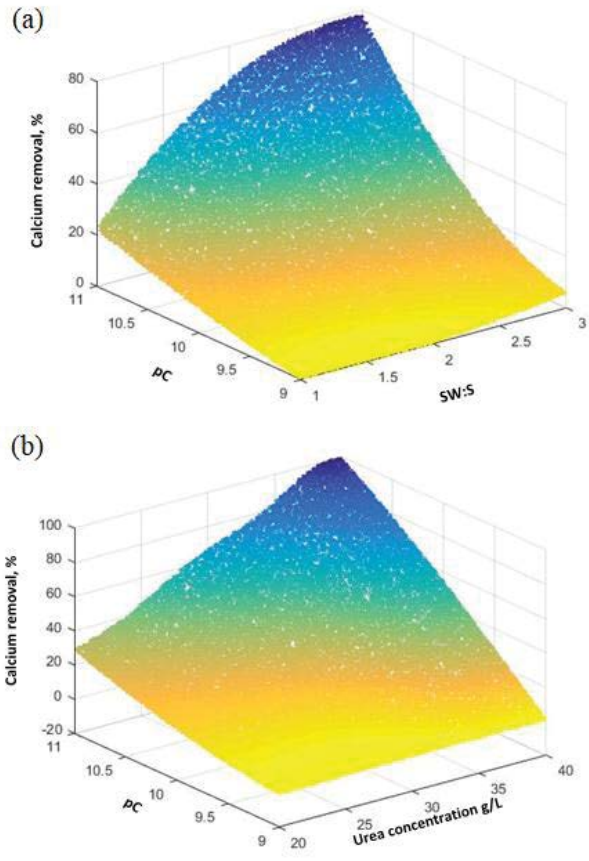

Fig. 9. The response surfaces for calcium removal. Urea concentration 30 g L^{-1} (a) and SW:S ratio 2 (b).

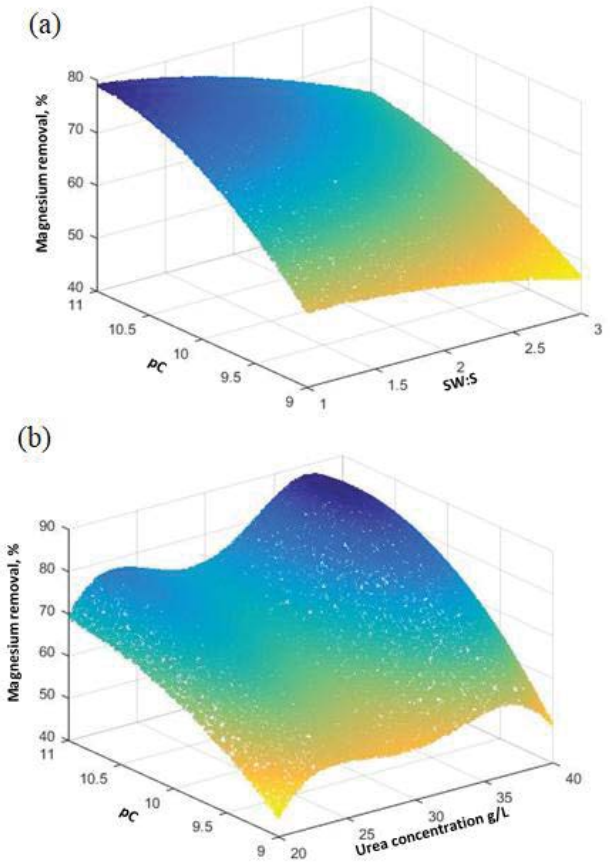

Fig. 10. The response surfaces for magnesium removal. Urea concentration 30 g L^{-1} (a) and SW:S ratio 2 (b).

(see Fig. 10). This suggests considering two reactors in series, the first with high values of SW:S to remove calcium and the second with low values of SW:S to remove magnesium. Further experimental and economic studies are needed given that optimal condition for calcium and magnesium removal are different and because the optimal condition (high level of urea) is not favorable from the economic point of view.

4. Conclusions

The removal of calcium and magnesium from SW was investigated considering the concentration of urea, number of cells in the immobilization matrix, and SW:S as independent variables. Based on an ANOVA analysis of a three-level factorial design it was determined that the input variable urea concentration, pC, and SW:S were highly significant in the removal of calcium. Also, the quadratic term of urea concentration, interaction urea concentration with pC, and interaction pC with SW:S ratio were significant in calcium removal. For magnesium removal, pC was the only highly significant variable, whereas the urea concentration, SW:S, and quadratic term of pC were significant.

The removal of calcium and magnesium were modeled using RSM and RBFN. It was demonstrated that RBFN gives superior results based on several metrics of accuracy.

Finally, the study demonstrated that immobilized cells of *B. subtilis* strain LN8B could be a promising method for partial removal of calcium and magnesium from SW.

Abbreviations

XRD, X-ray diffraction; SW, seawater; PVA-Al, Polyvinyl-alcohol-alginate; RSM, response surface methodology; ANNs, artificial neural networks; RBFN, radial basis function networks; SW:S, seawater to spheres ratio; RO, reverse osmosis; RMS, root mean square; MAE, mean absolute error; MRE, mean relative error.

Acknowledgments

This publication was supported by Anillo–Grant ACM 170005 (CONICYT), Ph.D. Scholarship CONICYT-PCHA/2013/21130712, CICITEM Project n° R10C1004 and the Regional Government of Antofagasta. The authors wish to thank Ana Cisternas for technical support.

References

[1] Association, I.D., Desalination by the Numbers | IDA, Available at: http://idadesal.org/desalination-101/desalination-by-the-numbers/ (accessed on Jan 1, 2017).
[2] U. Yermiyahu, A. Tal, A. Ben-Gal, A. Bar-Tal, J. Tarchitzky, O. Lahav, Rethinking desalinated water quality and agriculture, Science, 318 (2007) 920–921.
[3] F. Rahman, Calcium sulfate precipitation studies with scale inhibitors for reverse osmosis desalination, Desalination, 319 (2013) 79–84.
[4] A. Pérez-González, R. Ibáñez, P. Gómez, A.M. Urtiaga, I. Ortiz, J.A. Irabien, Recovery of desalination brines: separation of calcium, magnesium and sulfate as a pre-treatment step, Desal. Wat. Treat., 56 (2015) 3617–3625.
[5] S.T. Mitrouli, M. Kostoglou, A.J. Karabelas, A. Karanasiou, Incipient crystallization of calcium carbonate on desalination membranes: dead-end filtration with agitation, Desal. Wat. Treat., 57 (2016) 2855–2869.
[6] M. Khayet, Fouling and scaling in desalination, Desalination, 393 (2016) 1.
[7] D.M. Warsinger, J. Swaminathan, E. Guillen-Burrieza, H.A. Arafat, V.J. Lienhard, Scaling and fouling in membrane distillation for desalination applications: a review, Desalination, 356 (2015) 294–313.
[8] S.J. Pugh, G.F. Hewitt, H. Müller-Steinhagen, Fouling during the use of seawater as coolant – the development of a user guide, Heat Transfer Eng., 26 (2005) 35–43.
[9] M.S.H. Bader, Sulfate removal technologies for oil fields seawater injection operations, J. Pet. Sci. Eng., 55 (2007) 93–110.
[10] L.A. Cisternas, E.D. Gálvez, The use of seawater in mining, Miner. Process. Extr. Metall. Rev., 39 (2017) 18–33.
[11] R.I. Jeldres, L. Forbes, L.A. Cisternas, Effect of seawater on sulfide ore flotation: a review, Miner. Process. Extr. Metall. Rev., 37 (2016) 369–384.
[12] S. Castro, A. Lopez-Valdivieso, J.S. Laskowski, Review of the flotation of molybdenite. Part I: Surface properties and floatability, Int. J. Miner. Process., 148 (2016) 48–58.
[13] S. Castro, P. Rioseco, J.S. Laskowski, Depression of Molybdenite in Sea Water, XXVI Int. Miner. Process. Congr., 2012, pp. 737–752.
[14] R.I. Jeldres, M.P. Arancibia-Bravo, A. Reyes, C.E. Aguirre, L. Cortes, L.A. Cisternas, The impact of seawater with calcium and magnesium removal for the flotation of copper-molybdenum sulphide ores, Miner. Eng., 109 (2017) 10–13.
[15] J. Dick, W. De Windt, B. De Graef, H. Saveyn, P. Van Der Meeren, N. De Belie, W. Verstraete, Bio-deposition of a calcium carbonate layer on degraded limestone by *Bacillus* species, Biodegradation, 17 (2006) 357–367.

[16] A.J. Phillips, R. Gerlach, E. Lauchnor, A.C. Mitchell, A.B. Cunningham, L. Spangler, Engineered applications of ureolytic biomineralization: a review, Biofouling, 29 (2013) 715–733.
[17] G.A. Silva-Castro, I. Uad, A. Rivadeneyra, J.I. Vilchez, D. Martin-Ramos, J. González-López, M.A. Rivadeneyra, Carbonate precipitation of bacterial strains isolated from sediments and seawater: formation mechanisms, Geomicrobiol. J., 30 (2013) 840–850.
[18] S.M. Al-Thawadi, Ureolytic bacteria and calcium carbonate formation as a mechanism of strength enhancement of sand, J. Adv. Sci. Eng. Res., 1 (2011) 98–114.
[19] S.M. Al-Thawadi, Consolidation of sand particles by aggregates of calcite nanoparticles synthesized by ureolytic bacteria under non-sterile conditions, J. Chem. Sci. Technol., 2 (2013) 141–146.
[20] F. Hammes, K. Van Hege, T. Van De Wiele, J. Vanderdeelen, S.D. Siciliano, W. Verstraete, Calcium removal from industrial wastewater by bio-catalytic $CaCO_3$ precipitation, J. Chem. Technol. Biotechnol., 78 (2003) 670–677.
[21] M. Carballa, W. Moerman, W. De Windt, H. Grootaerd, W. Verstraete, Strategies to optimize phosphate removal from industrial anaerobic effluents by magnesium ammonium phosphate (MAP) production, J. Chem. Technol. Biotechnol., 84 (2006) 63–68.
[22] L. Altaş, A. Kiliç, H. Koçyiğit, M. Işik, Adsorption of Cr(VI) on ureolytic mixed culture from biocatalytic calcification reactor, Colloids Surf., B, 86 (2011) 404–408.
[23] E. Desmidt, K. Ghyselbrecht, A. Monballiu, W. Verstraete, B.D. Meesschaert, Evaluation and thermodynamic calculation of ureolytic magnesium ammonium phosphate precipitation from UASB effluent at pilot scale, Water Sci. Technol., 65 (2012) 1954–1962.
[24] M. Işık, L. Altaş, S. Özcan, İ. Şimşek, O.N. Ağdağ, A. Alaş, Effect of urea concentration on microbial Ca precipitation, J. Ind. Eng. Chem., 18 (2012) 1908–1911.
[25] D. Arias, D.L.A. Cisternas, M. Rivas, Biomineralization of calcium and magnesium crystals from seawater by halotolerant bacteria isolated from Atacama Salar (Chile), Desalination, 405 (2017) 1–9.
[26] G.D.O. Okwadha, J. Li, Optimum conditions for microbial carbonate precipitation, Chemosphere, 81 (2010) 1143–1148.
[27] L.S. Wong, Microbial cementation of ureolytic bacteria from the genus *Bacillus*: a review of the bacterial application on cement-based materials for cleaner production, J. Cleaner Prod., 93 (2015) 5–17.
[28] G.I. Danmaliki, T.A. Saleh, A.A. Shamsuddeen, Response surface methodology optimization of adsorptive desulfurization on nickel/activated carbon, Chem. Eng. J., 313 (2017) 993–1003.
[29] K.N. Kontogiannopoulos, S.I. Patsios, A.J. Karabelas, Tartaric acid recovery from winery lees using cation exchange resin: optimization by response surface methodology, Sep. Purif. Technol., 165 (2016) 32–41.
[30] A. Zuorro, Optimization of polyphenol recovery from espresso coffee residues using factorial design and response surface methodology, Sep. Purif. Technol., 152 (2015) 64–69.
[31] F. Charte, I. Romero, M.D. Pérez-Godoy, A.J. Rivera, E. Castro, Comparative analysis of data mining and response surface methodology predictive models for enzymatic hydrolysis of pretreated olive tree biomass, Comput. Chem. Eng., 101 (20017) 23–30.
[32] V.M. Simić, K.M. Rajković, S.S. Stojičević, D.T. Veličković, N.Č. Nikolić, M.L. Lazić, I.T. Karabegović, Optimization of microwave-assisted extraction of total polyphenolic compounds from chokeberries by response surface methodology and artificial neural network, Sep. Purif. Technol., 160 (2016) 89–97.
[33] D.A.D. Genuino, B.G. Bataller, S.C. Capareda, M.D.G. de Luna, Application of artificial neural network in the modeling and optimization of humic acid extraction from municipal solid waste biochar, J. Environ. Chem. Eng., 5 (2017) 4101–4107.
[34] A. Aminian, Prediction of temperature elevation for seawater in multi-stage flash desalination plants using radial basis function neural network, Chem. Eng. J., 162 (2010) 552–556.
[35] S. Uchimurai, Y. Hamamotoj, S. Tomitat, Effects of the Sample Size in Artificial Neural Network Classifier Design, Proc. ICNN'95 - International Conference on Neural Networks, IEEE, vol. 4, 1995, pp. 2126–2129.
[36] A. Idri, A. Zakrani, A. Zahi, Design of radial basis function neural networks for software effort estimation, Int. J. Comput. Sci., 7 (2010) 11–17.
[37] G. Delgado, R. Delgado, J. Párraga, M.A. Rivadeneyra, V. Aranda, Precipitation of carbonates and phosphates by bacteria in extract solutions from a semi-arid saline soil. Influence of Ca^{2+} and Mg^{2+} concentrations and Mg^{2+}/Ca^{2+} molar ratio in biomineralization, Geomicrobiol. J., 25 (2008) 1–13.
[38] K.S. Le Corre, E. Valsami-Jones, P. Hobbs, S.A. Parsons, Impact of calcium on struvite crystal size, shape and purity, J. Cryst. Growth, 283 (2005) 514–522.